The R-Ras interaction partner ORP3 regulates cell adhesion

Markku Lehto[1,2], Mikko I. Mäyränpää[3,4], Teijo Pellinen[5], Pekka Ihalmo[2], Sanna Lehtonen[6], Petri T. Kovanen[3], Per-Henrik Groop[2], Johanna Ivaska[5] and Vesa M. Olkkonen[1,*]

[1]Department of Molecular Medicine, National Public Health Institute, Biomedicum, FI-00251 Helsinki, Finland
[2]Folkhälsan Institute of Genetics, Folkhälsan Research Centre Biomedicum, Biomedicum, University of Helsinki, Helsinki, Finland
[3]Wihuri Research Institute, Helsinki, Finland
[4]Department of Forensic Medicine, University of Helsinki, Finland
[5]VTT Medical Biotechnology, Turku, Finland
[6]Department of Pathology, Haartman Institute, University of Helsinki, Finland
*Author for correspondence (e-mail: vesa.olkkonen@ktl.fi)

Accepted 19 November 2007
Journal of Cell Science 121, 695-705 Published by The Company of Biologists 2008
doi:10.1242/jcs.016964

Summary

Oxysterol-binding protein (OSBP)-related protein 3 (ORP3) is highly expressed in epithelial, neuronal and hematopoietic cells, as well as in certain forms of cancer. We assessed the function of ORP3 in HEK293 cells and in human macrophages. We show that ORP3 interacts with R-Ras, a small GTPase regulating cell adhesion, spreading and migration. Gene silencing of *ORP3* in HEK293 cells results in altered organization of the actin cytoskeleton, impaired cell-cell adhesion, enhanced cell spreading and an increase of β1 integrin activity – effects similar to those of constitutively active R-Ras(38V). Overexpression of ORP3 leads to formation of polarized cell-surface protrusions, impaired cell spreading and decreased β1 integrin activity. In primary macrophages, overexpression of ORP3 leads to the disappearance of podosomal structures and decreased phagocytotic uptake of latex beads, consistent with a role in actin regulation. ORP3 is phosphorylated when cells lose adhesive contacts, suggesting that it is subject to regulation by outside-in signals mediated by adhesion receptors. The present findings demonstrate a new function of ORP3 as part of the machinery that controls the actin cytoskeleton, cell polarity and cell adhesion.

Supplementary material available online at
http://jcs.biologists.org/cgi/content/full/121/5/695/DC1

Key words: Actin cytoskeleton, Cell adhesion, Cell polarization, Cell spreading, HEK293, Macrophages, Oxysterol-binding protein, R-Ras

Introduction

The human oxysterol-binding protein (OSBP)-related protein (ORP) family consists of 12 members (OSBP, ORP1-ORP11) (Lehto et al., 2001; Jaworski et al., 2001). The ORPs are characterized by a C-terminal OSBP-related ligand-binding domain (ORD), which binds oxidized cholesterol derivatives and possibly other unidentified ligands. Most ORPs have an N-terminal pleckstrin-homology (PH) domain, which mediates binding of membrane phosphoinositides. This conserved structure plays an important role in the intracellular targeting of ORPs. In addition, 8 out of the 12 ORPs carry a FFAT (two phenylalanines in an acidic tract) motif, which enables these proteins to interact with VAMP-associated protein A (VAP-A) at the endoplasmic reticulum (ER). Based on the current data, ORPs are involved in the regulation of lipid metabolism, vesicle transport and cell signaling. It is, however, unclear whether ORPs function as sterol transporters or signaling molecules in these cellular processes (Lehto and Olkkonen, 2003; Olkkonen et al., 2006)

The highly homologous ORP3, ORP6 and ORP7 proteins belong to ORP subfamily III (Lehto et al., 2001). Based on the analysis of structural features and subcellular localization, these proteins were suggested to be involved in communication between the ER and plasma membrane (Lehto et al., 2004). Members of subfamily III show distinct expression patterns suggesting tissue-specific aspects of their function: ORP3 (kidney, lymphatic tissues), ORP6 (brain, skeletal muscle) and ORP7 (gastrointestinal tract) (Lehto et al., 2004). High levels of *ORP3* mRNA expression in blood leukocytes, such as B-cells, T-cells and macrophages have also been observed (Johansson et al., 2003; Tuomisto et al., 2005) (M. Lehto and V.M.O., unpublished observations). Moreover, ORP3 expression was found to be upregulated in malignancies, such as Burkitt's lymphoma and colorectal adenocarcinoma (Lehto et al., 2004). Analysis of chromosomal abnormalities has revealed that the *ORP3* (*OSBPL3* – HGNC database) gene region in chromosome 7 is often gained and overexpressed in colon tumors and osteosarcoma (Ozaki et al., 2003; Staub et al., 2006; Tsafrir et al., 2006). Increased expression of *ORP3* mRNA has frequently been reported in B-cell-associated malignancies (Ando et al., 2003; Sander et al., 2005; Chng et al., 2006; Ek et al., 2006) and testicular cancer (Sperger et al., 2003; Yamada et al., 2004; Almstrup et al., 2005; Gashaw et al., 2005; Juric et al., 2005). In a prospective study of patients with diffuse large B-cell lymphoma (DLBCL), high ORP3 expression was associated with increased mortality (Ando et al., 2003). In hematopoietic cells, unfavorable retroviral integrations may trigger leukemia. The *ORP3* gene was identified as one of the common insertion sites of Moloney murine leukemia virus (MMLV) in a mouse model of B-cell leukemia (Bijl et al., 2005). These observations indicate that ORP3 could play an important role in certain forms of cancer.

In the present study, we investigated the function of ORP3 in the embryonic kidney cell line HEK293 and in primary

macrophages, both of which express endogenous ORP3 at high levels (Lehto et al., 2004). The present findings show that ORP3 interacts with the small GTPase R-Ras and demonstrate a new functional role of ORP3 as part of the machinery that controls the actin cytoskeleton, cell polarity and cell adhesion.

Results

Localization of the endogenous ORP3 in HEK293 cells

In preliminary analyses we found that ORP3 is expressed at high levels in kidney tubule epithelia (supplementary material Fig. S1) and in the human embryonic kidney cell line HEK293, which was chosen as a model system to study the subcellular localization and function of ORP3. The endogenous ORP3 protein in HEK293 cells colocalized significantly with protein disulphide isomerase (PDI) at the endoplasmic reticulum (ER; data not shown). At the plasma membrane, anti-ORP3 antibodies stained thin filopodial cell-surface projections (Fig. 1A-C). In some cells, especially those with thicker and longer protrusions, ORP3 concentrated at the very tips of these extensions (Fig. 1D-F). The ORP3-positive cell-surface projections were frequent in subconfluent cultures, but disappeared almost entirely when HEK293 cells were plated at high cell density, resulting in abundant cell-cell contacts (Fig. 1G-I). The staining patterns described are specific for ORP3, because the reactivity was inhibited by pre-incubation of anti-ORP3 antibodies with the immunizing peptide (Fig. 1J-L).

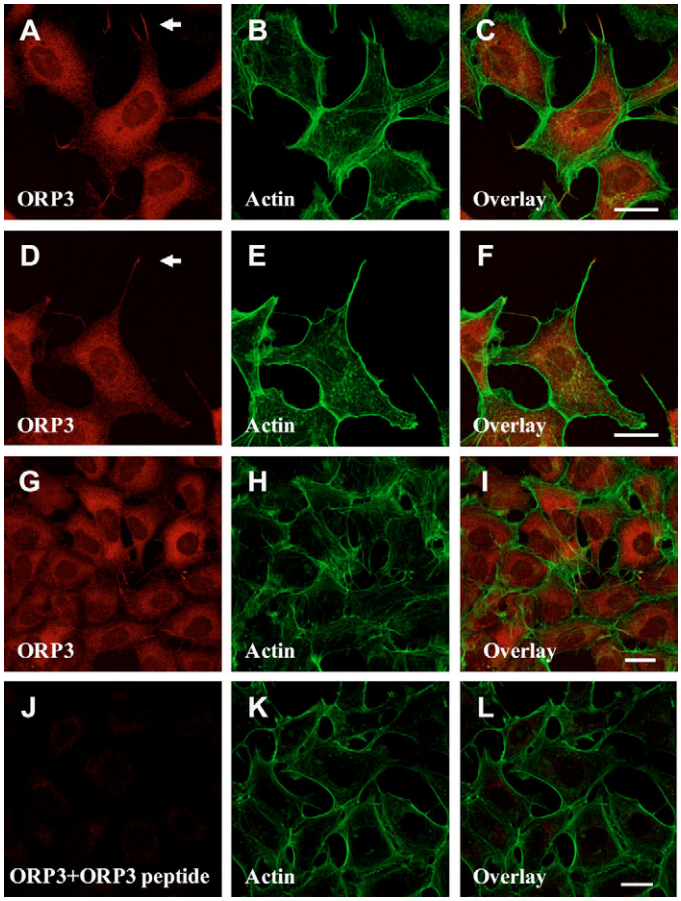

Fig. 1. Localization of endogenous ORP3 in HEK293 cells. Immunofluorescence microscopy analysis of HEK293 cells using anti-ORP3 antibodies. F-actin was stained with OG488P. The arrows in A and D indicate ORP3 staining at the filopodial plasma membrane extensions. The low-magnification views (G-I) visualize the loss of ORP3-positive filopodia in cultures of increased cell density. Specificity of the staining pattern is demonstrated by preincubation of the ORP3 antibody with the immunizing peptide, leading to loss of the immunoreactivity (J-L). Scale bars: 20 μm.

ORP3 overexpression induces polarized cell-surface protrusions in HEK293 cells

To address the effects of ORP3 overexpression on cell morphology, HEK293 cells were transfected with ORP3 expression plasmid constructs. At 20 hours after transfection, most of the ORP3-expressing cells displayed one or two long protrusions. The overexpressed ORP3 itself was distributed in the cytoplasm and in the oval-shaped tips of the protrusion ends (Fig. 2A-C). This phenotype was not restricted to HEK293 cells; overexpression of ORP3 protein induced similar protrusions in the MCF-7 breast cancer cell line (data not shown).

We next tested which part of the ORP3 protein was responsible for the protrusion phenotype. For this purpose, we used previously generated mutated and truncated *ORP3* cDNA constructs (supplementary material Fig. S2). Inactivation of the FFAT (ORP3mFFAT) motif had no significant influence on the frequency or shape of ORP3-induced protrusions (Fig. 2D-F). Disruption of the PH domain (ORP3mPH2), however, markedly inhibited the protrusion phenotype (Fig. 2G-I). The PH domain required for the plasma membrane targeting of ORP3 (Lehto et al., 2005) thus seems to play an important role in formation of the protrusions. This observation is supported by data with another ORP3 construct, FR1(398-886), which lacks the N-terminal region harboring the PH domain. The protrusion phenotype was severely inhibited in cells transfected with this construct. Instead of protrusions, many of the transfected cells had an increased number of shorter projections on the cell surface (Fig. 2J-L). The C-terminally truncated construct, FR6(1-555), which lacks most of the C-terminal OSBP-related domain, was also capable of inducing cell-surface protrusions (Fig. 2M-O). Of note, FR6(1-555)-transfected cells often displayed more branched and elongated protrusions than those induced by wild-type ORP3. This finding is consistent with the fact that the OSBP-related domain has a negative regulatory effect on the activity of the PH domain (Lehto et al., 2005).

ORP3 interacts with R-Ras

A putative interaction between constitutively active R-Ras(38V) and ORP3 in mouse fibroblasts was recently detected in a study using tandem affinity-tagged R-Ras(38V) (Goldfinger et al., 2007). We therefore tested whether ORP3 could be coimmunoprecipitated with wild-type R-Ras(wt), the constitutively active mutant R-Ras(38V) or the dominant negative mutant R-Ras(43N). As shown in Fig. 3A, ORP3 precipitated at a similar efficiency with all three forms of R-Ras. No ORP3 was detected in precipitates obtained with control rabbit IgG. To obtain clues of a possible functional interplay between the two proteins, we tested how coexpression of the three forms of R-Ras affects the protrusion phenotype induced by ORP3. Although R-Ras(wt) and R-Ras(38V) failed to modify the ORP3 phenotype, the inhibitory R-Ras(43N) mutant inhibited formation of the protrusions and resulted in an increased number of filopodial cell-surface extensions (Fig. 3B). Consistent with the observed interaction of ORP3 and R-Ras, immunofluorescence microscopy analysis of HEK293 cells revealed colocalization of the endogenous ORP3 and R-Ras proteins especially at the ends of

protrusive cell extensions, which were occasionally also observed in untransfected cells (Fig. 3C).

Gene silencing of *ORP3* impacts on the actin cytoskeleton and cell spreading

To address ORP3 function in HEK293 cells, we transfected the cells with control (siC1) or *ORP3*-specific siRNAs. The *ORP3* siRNAs induced a significant (>80%) downregulation of the gene product (Fig. 4A). The cells were trypsinized and plated on fibronectin-coated coverslips to allow spreading at low cell density. At the earliest time points (20-40 minutes), untreated and siC1-transfected cells displayed small bodies with numerous extending projections (Fig. 4B). The cells subjected to *ORP3* silencing showed a very distinct phenotype. They had fewer projections, which were embedded within extending lamellipodia. At 2 hours after plating, the untransfected and control siRNA-treated cells displayed compact cortical actin staining at the cell periphery, whereas the siORP3-treated cells showed 'basket-like' networks of actin filaments (Fig. 4B). This phenotype seemed to correlate with the level of *ORP3* expression. Some of the si*ORP3*-transfected cells, which expressed ORP3 protein at higher levels, displayed actin staining similar to control cells (arrow in Fig. 4C). The ability of ORP3 and R-Ras to regulate the cytoskeleton was further supported by the fact that R-Ras(38V) expression alone induced a similar actin phenotype as that seen in HEK293 cells subjected to *ORP3* gene silencing (Fig. 4D).

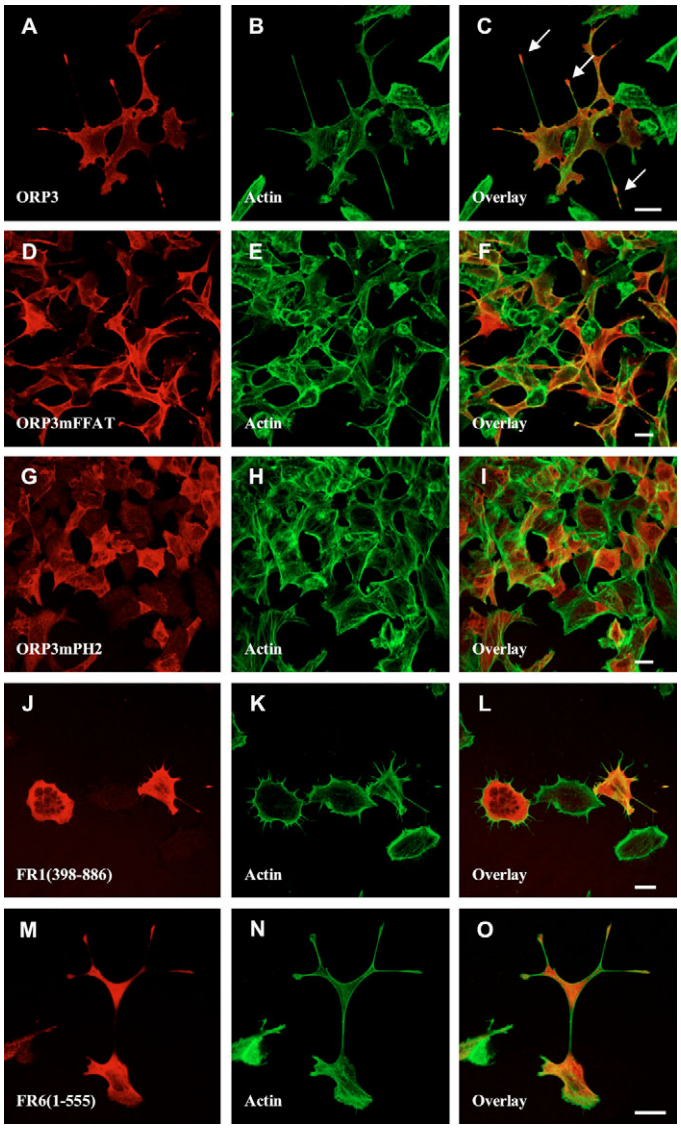

Fig. 2. ORP3 overexpression induces cell-surface protrusions in HEK293 cells. HEK293 cells were transfected with N-terminally Xpress-tagged *ORP3* plasmid constructs. At 20 hours post transfection, the cells were fixed and stained using anti-Xpress™ antibodies. F-actin was visualized with OG488P. (A-C) Wild-type ORP3 (protrusions indicated by arrows), (D-F) ORP3mFFAT, (G-I) ORP3mPH2, (J-L) FR1(398-886), (M-O) FR6(1-555). Scale bars: 20 μm.

Since *ORP3* gene silencing had a clear impact on the morphology of the spreading cells, we assessed quantitatively whether decreased or increased expression of ORP3 influences the cell-spreading process. After transfection with siRNA or plasmid constructs, HEK293 cells were trypsinized and replated on fibronectin-coated coverslips for 1 hour and the spreading area of the cells was quantified. Compared with controls, the area of si*ORP3*-transfected cells was increased by 50% ($P<0.001$; Fig. 5A). Overexpression of ORP3 had the opposite effect: cell area was decreased by 15% compared with that in mock-transfected controls ($P<0.001$).

To gain insight into the mechanisms by which ORP3 could affect the cell-spreading process, we tested whether ORP3 plays a role in cell adhesion or the regulation of the active conformation of cells surface β1 integrins. Loss-of-function experiments showed that ORP3 plays an inhibitory role in cell adhesion; gene silencing of *ORP3* increased cell adhesion to collagen (Fig. 5B) and fibronectin (not shown) approximately twofold ($P<0.001$). Interestingly, ORP3 overexpression decreased integrin activity by 22% ($P<0.05$) compared with mock-transfected cells, whereas silencing of *ORP3* increased the level of active integrin on the cell surface by 24% ($P<0.01$) (Fig. 5C). The expression of si*ORP3*-resistant *ORP3* cDNA construct (ORP3mut/pcDNA4) fully reversed the integrin-activating effect of *ORP3* siRNA, confirming that ORP3 functions as a negative regulator of integrin activity (Fig. 5D).

The functional connection between R-Ras and ORP3 was addressed by investigating the effects of R-Ras expression in cells subjected to *ORP3* gene silencing. Expression of wild-type R-Ras and constitutively active R-Ras(38V) were both able to induce a further increase in integrin activity compared with *ORP3* gene silencing alone (Fig. 5E). Conversely, dominant-negative R-Ras(43N) was able to attenuate the integrin activity in *ORP3*-silenced cells. Immunofluorescence analysis of cells from the same transfections revealed that the R-Ras mutants induce changes in the cytoskeleton independently of ORP3 expression. These data suggest that R-Ras is downstream of ORP3 or on a separate pathway with respect to regulation of integrin activity and changes in the actin cytoskeleton.

ORP3 gene silencing inhibits cell-cell adhesion

To assess the effect of *ORP3* gene silencing on cell-cell adhesion, HEK293 cells were treated with control or *ORP3*-specific siRNAs for 3 days, during which time the cells reached confluency. The cell-cell contacts were visualized using pan-cadherin and β-catenin antibodies. Cells treated with control siRNA were surrounded by continuous lines of β-catenin and cadherin staining (Fig. 6A-D). In cultures subjected to *ORP3* silencing, a majority of the cell-cell contact staining was lost (Fig. 6E-H). Of note, endogenous ORP3 itself was not found in the zones of cell-cell contact (see Fig. 1).

The functional effects of ORP3 overexpression in primary macrophages

In addition to its expression in the epithelia of several tissues (supplementary material Fig. S1), ORP3 is expressed at high levels in leukocytes, including CD68$^+$ macrophages in lymph nodes, sites of foreign body reaction (not shown) and atherosclerotic lesions (supplementary material Fig. S1). We therefore assessed the effect of ORP3 overexpression on the actin cytoskeleton and the phagocytic process in primary human monocyte macrophages. The cells were infected with recombinant adenoviruses expressing ORP3 (Ad*ORP3*) or GFP only (Ad*GFP*) for 72 hours. Typical podosomal structures were seen upon F-actin staining of the Ad*GFP*-infected macrophages (Fig. 7A-C). In Ad*ORP3*-transduced cells, disturbed actin morphology was accompanied by a total loss of podosomes (Fig. 7D-F). Furthermore, we tested the functional effect of ORP3 overexpression on macrophage phagocytosis activity. Monocyte-macrophages derived from three different blood donors were infected with Ad*ORP3* and Ad*GFP* for 3 days, followed by incubation with 3 μm polystyrene latex beads for 1 hour (Fig. 7G). The Ad*ORP3*-transduced macrophages (n=385) contained significantly fewer internalized latex beads than the Ad*GFP*-infected control cells (n=885) (3.6 vs 5.5 beads/cell; P=0.001), demonstrating a disturbance of the phagocytic process. Whether this is due to a defect in binding of the beads on the cell surface or in the actual phagocytic internalization process cannot be stated based on the present data.

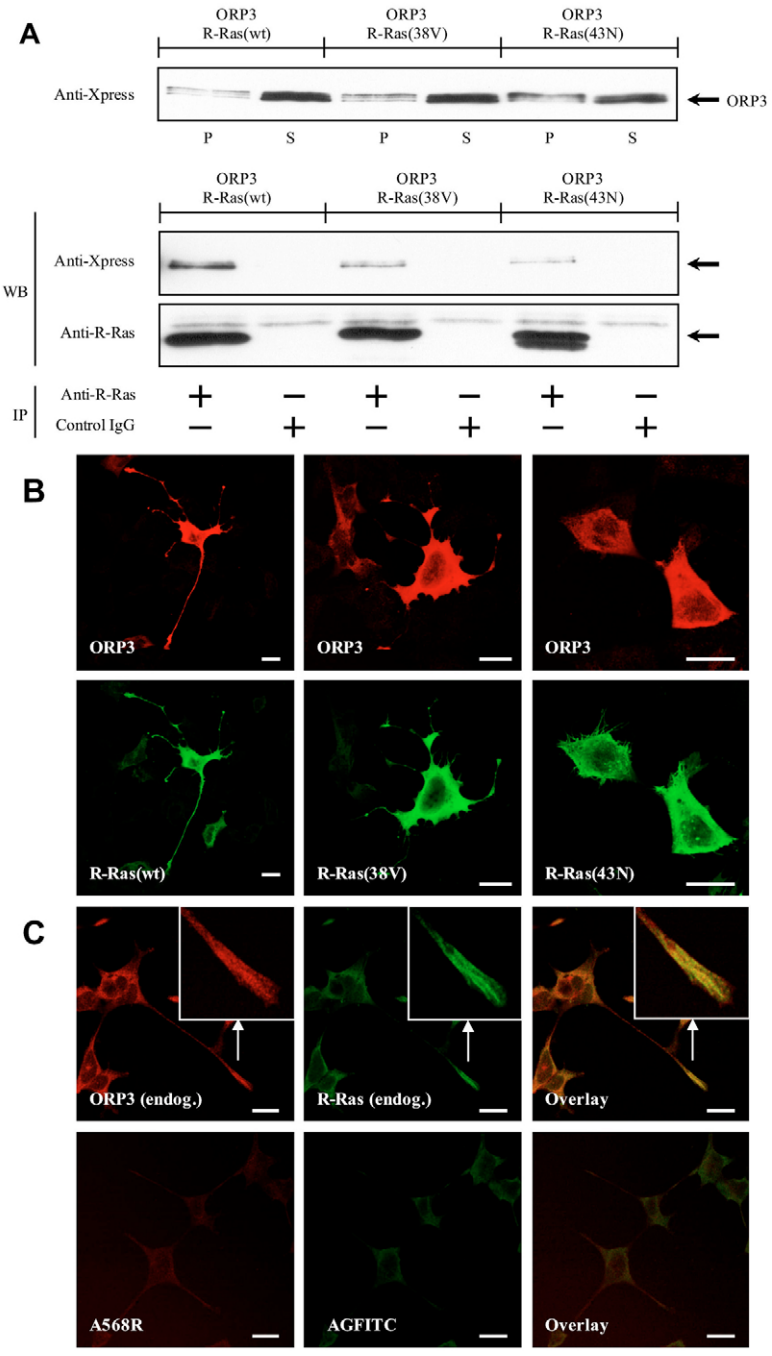

Fig. 3. ORP3 interacts with R-Ras. (A) HEK293 cells doubly transfected with *ORP3*/R-Ras(wt), *ORP3*/R-Ras(38V) or *ORP3*/R-Ras(43N) cDNA constructs were lysed in detergent-containing buffer, followed by removal of insoluble material by centrifugation. The insoluble pellets (P) and the soluble fractions (S) are depicted in the top panel. The S fractions were subjected to immunoprecipitation (IP) with anti-R-Ras or irrelevant control (Control IgG) rabbit antibodies. ORP3 and R-Ras in the immunocomplexes were visualized by western blotting (WB) using anti-Xpress™ and anti-R-Ras antibodies, respectively. (B) HEK293 cells doubly transfected with the *ORP3* cDNA and with R-Ras(wt), the constitutively active R-Ras(38V), or with the dominant inhibitory R-Ras(43N) and stained with anti-ORP3 and anti-R-Ras antibodies. (C) Untransfected HEK293 cells double-stained for endogenous ORP3 and R-Ras. The inset shows a magnified view of a protrusion end. The bottom panels display a similar specimen treated with the secondary antibody conjugates only, anti-rabbit Alexa Fluor 568 (A568R) and anti-goat-FITC (AGFITC), to demonstrate specificity of the staining patterns. Scale bars: 20 μm.

ORP3 is phosphorylated is response to loss of cell adhesion

The anti-ORP3 antibodies detected two closely located protein bands with the apparent molecular masses of 103 and 110 kDa in western analysis of HEK293 cells. Initially, it was uncertain whether these bands represented alternatively spliced or post-translationally modified ORP3 protein products. HEK293 cells were trypsinized briefly and plated again on fibronectin-coated dishes for 1 hour in the presence of normal medium. In western analysis, the replated cells had a clearer and stronger upper band than adherent cells, which had been on the dishes for more than 20 hours (Fig. 8A, first two lanes). In time-course experiments we monitored the band shift in RP cells for 120 minutes after replating. The shift was maximal already at the 20-minute time point and no further change was observed over a further 2 hours (Fig. 8B). The rapid time scale of the ORP3 band shift suggested that the phenomenon is not due to differential splicing but rather reflects a post-translational modification, most likely a change in phosphorylation. To investigate this, we first tested the effects of the protein kinase C activators phorbol myristate acetate (PMA) and all-trans retinoic acid (ATRA), on the ORP3 band shift. A 1-hour treatment with PMA induced a strong upper band in both adherent and replated cells. Treatment with ATRA had a similar albeit weaker effect (Fig. 8A). Next we tested whether treatment of cell lysates with lambda protein phosphatase (λ-PPase; a

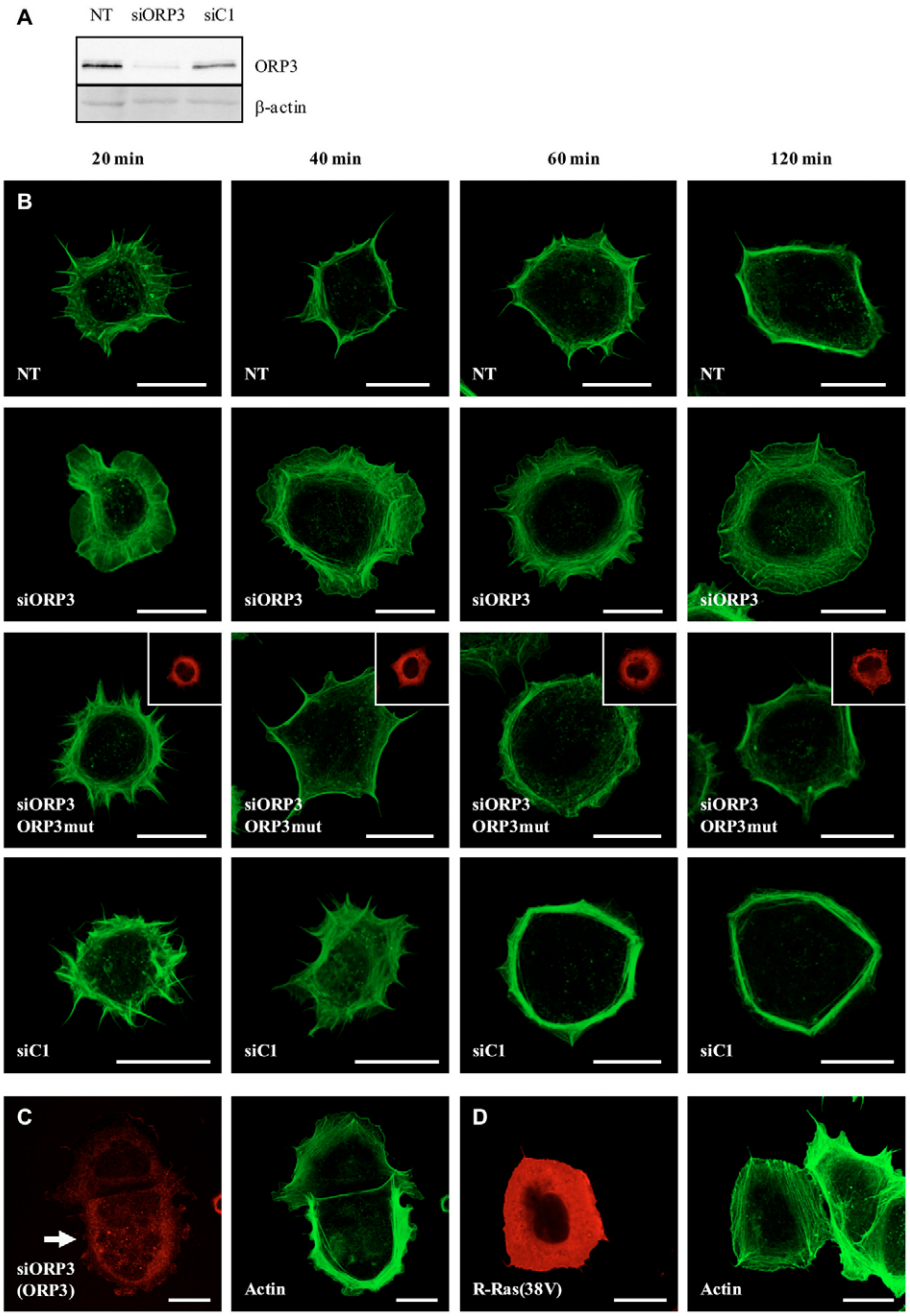

Fig. 4. Effects of *ORP3* gene silencing on the actin cytoskeleton and HEK293 cell morphology. (A) Western blot analysis of ORP3 protein in HEK293 cells (NT) and cells treated with si*ORP3* or siC1 siRNAs twice over a 3-day period. (B) HEK293 cells transfected with the indicated siRNAs, or cotransfected with si*ORP3* and a resistant mutant *ORP3* cDNA (ORP3mut), were trypsinized, replated on fibronectin-coated coverslips and allowed to spread for 20, 40, 60 and 120 minutes (as indicated) in the presence of normal culture medium. The F-actin was stained using OG488P. The insets in the si*ORP3* *ORP3*mut specimens, stained with anti-ORP3, verify expression of the *ORP3* mutant cDNA in the imaged cells. (C) si*ORP3*-transfected cells at the 120 minute time point. The arrow indicates a cell that expresses ORP3 protein at a higher level than the neighbouring cells. (D) R-Ras(38V)-transfected cell at the 120 minute time point of a spreading experiment. Scale bars: 20 μm.

Mn^{2+}-dependent protein phosphatase with activity towards phosphorylated serine, threonine and tyrosine residues) influences the intensity of ORP3-positive protein bands. Indeed, treatment of adherent and replated cell lysates with λ-PPase resulted in a complete band shift to the lower position (Fig. 8C). Okadaic acid is a potent inhibitor of serine/threonine protein phosphatases type 1 (PP1) and 2A (PP2A). Treatment of adherent HEK293 cells with okadaic acid for increasing times induced a gradual increase in the upper band intensity, which was, after 2 hours, approximately threefold that of the starting level (Fig. 8D). These observations provide strong evidence that the upper band represents a phosphorylated form of ORP3. Interestingly, treatment of HEK293 cells with PMA resulted in the formation of protrusions that displayed endogenous ORP3 concentrated at their tips (supplementary material Fig. S3). In addition, the okadaic-acid-treated cells displayed an increased number of ORP3-positive filopodial extensions, indicating that changes in the phosphorylation status of ORP3 may modify its subcellular distribution.

Next, we tested whether the phosphorylation of ORP3 is dependent on cell-matrix and/or cell-cell adhesion. A significant increase in upper band intensity was evident immediately after brief trypsinization (Fig. 8E), indicating that ORP3 is phosphorylated rapidly upon loss of cell adhesion to neighbouring cells and matrix. A similar result was obtained when trypsinized cells were incubated for 1 hour in wells treated with denatured BSA to inhibit adhesion (Fig. 8F). To investigate whether cell-cell contacts are involved, equal numbers of HEK293 cells were plated on 3 cm and 10 cm dishes. On the following day, the phosphorylation status of the ORP3

protein was analyzed. Samples from subconfluent 10 cm plates (40-60%) displayed increased ORP3 phosphorylation, whereas the dephosphorylated form of ORP3 was predominant in samples derived from fully confluent (AD) 3 cm dishes (Fig. 8G). These results show that ORP3 phosphorylation is not only dependent on loss of matrix adhesion, but also correlates negatively with the extent of cell-cell contacts.

We next assessed whether disruption of cell-cell contacts stimulates ORP3 phosphorylation. Treatment of confluent HEK293 cells with 5 mM EGTA resulted in disruption of cell-cell contacts but no detachment of the cells from the substratum (supplementary material Fig. S4). The loss of cell-cell contacts coincided with a clear increase of ORP3 phosphorylation (Fig. 8H). E-cadherin plays a central role in the establishment of Ca^{2+}-dependent cell-cell adhesions (Wheelock and Johnson, 2003). Intriguingly, incubation of confluent HEK293 cells with an E-cadherin antibody (DECMA-1) increased ORP3 phosphorylation to a similar extent as the EGTA treatment (Fig. 8H), even though the cell-cell contacts remained intact (supplementary material Fig. S4).

Discussion

ORP3 belongs to a family of OSBP-related proteins (ORPs), which are thought to be involved in the regulation of cellular lipid metabolism, vesicle transport and cell signaling. All 12 human ORPs have distinct tissue-specific expression patterns (Lehto et al., 2001). The aim of the present study was to investigate ORP3 function in cells that express it endogenously at high levels. For this purpose, we selected the human embryonic kidney HEK293 cell line and primary macrophages. In the present study, we show that: (1) ORP3 interacts with the small GTPase R-Ras; (2) ORP3 regulates cell-matrix and cell-cell adhesion; (3) ORP3 expression has a marked impact on the actin cytoskeleton; and (4) phosphorylation of ORP3 is dependent on cell adhesion.

The finding that human ORP3 interacts with the small GTPase R-Ras is consistent with a recent investigation reporting the identification of ORP3 and its closest homolog ORP7 as binding partners of tandem affinity purification (TAP)-tagged R-Ras(38V) in murine fibroblasts (Goldfinger et al., 2007). Active R-Ras promotes integrin activity and stimulates the adhesive properties of

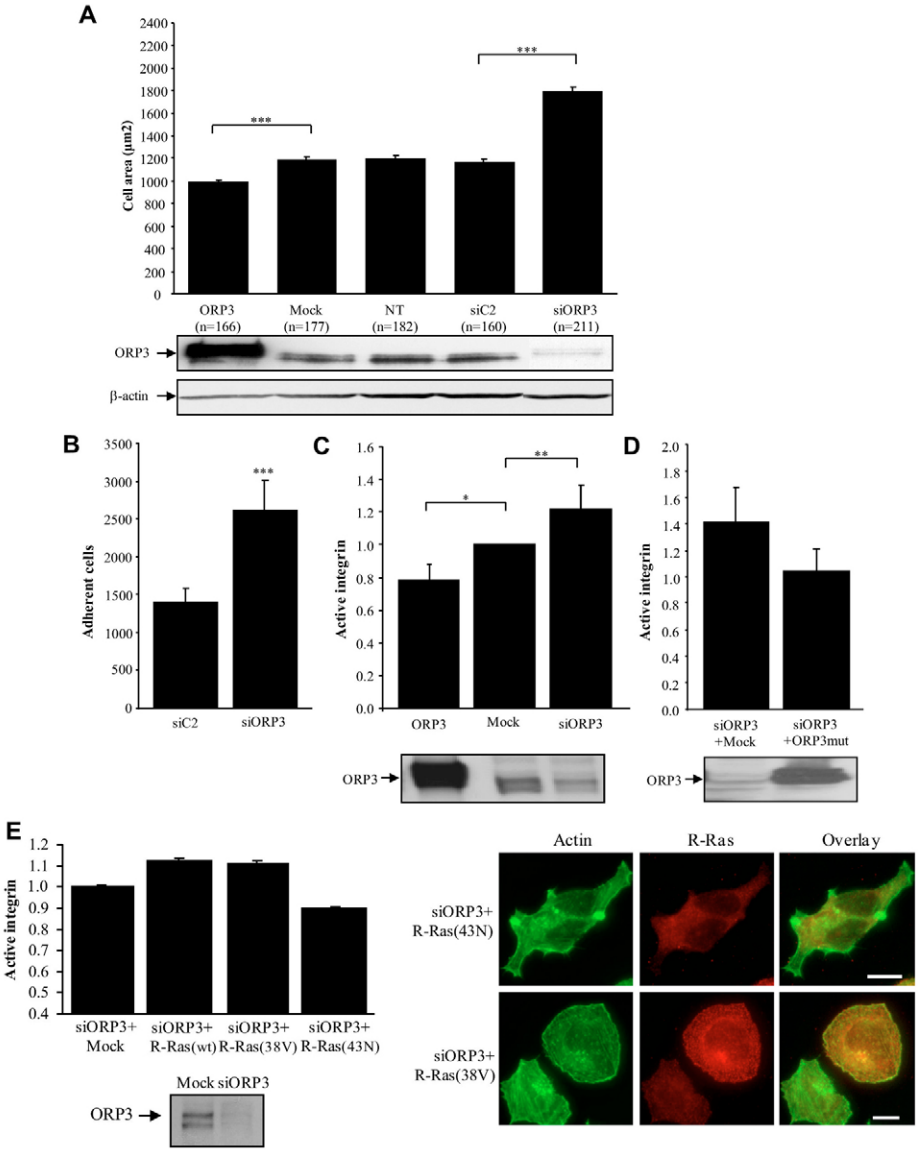

Fig. 5. ORP3 regulates HEK293 cell adhesion, spreading and β1 integrin activity. (A) Effect of *ORP3* overexpression and silencing on cell spreading. HEK293 cells were transfected with *ORP3* cDNA, with the empty vector (Mock), or with *ORP3*-specific (siORP3) or control (siC2) siRNAs. NT, non-transfected cells. Trypsinized cells were plated on fibronectin-coated coverslips for 1 hour, fixed and stained with OG488P. The area covered by the cells was determined from confocal microscope images. The figure shows mean area (± s.e.m.) of cells analysed from three different coverslips in the same experiment. The total numbers of cells analyzed are indicated. The expression levels of ORP3 and β-actin were assayed by western blotting of 20 µg total cell protein (2 µg for the *ORP3*-transfected specimen). (B) Effect of *ORP3* silencing on cell adhesion on substratum. HEK293 cells treated with siC2 or si*ORP3* were trypsinized, allowed to adhere on collagen substratum for 1 hour and the number of adherent cells was determined. (C) ORP3 modulates β1 integrin activity. The amount of active integrin in cells transfected with *ORP3* cDNA (ORP3), empty plasmid (Mock), or *ORP3* siRNA was determined by FACS analysis using P4G11 antibody, which recognizes active β1 integrin. The amount of active integrin was calculated relative to total β1 integrin (P5D2 antibody) expressed on the cell surface. (D) Rescue of the *ORP3*-silencing phenotype. HEK293 cells were transfected with empty plasmid and *ORP3* siRNA (siORP3+mock) or *ORP3* mutant cDNA resistant to the siRNA and *ORP3* siRNA (siORP3+ORP3mut), followed by analysis of the amount of active integrin on the cell surface. Western blot panels verify successful ORP3 overexpression and silencing. The results represent mean ± s.e.m.; **P*<0.05; ***P*<0.01; ****P*<0.001. (E) R-Ras regulates integrins downstream of ORP3. HEK293 cells transiently transfected with empty plasmid and *ORP3* siRNA (siORP3+mock) or *ORP3* siRNA and R-Ras constructs, were studied for integrin activity as above, or were allowed to spread on fibronectin-coated coverslips for 120 minutes, fixed and stained as indicated. Scale bars, 10 µm.

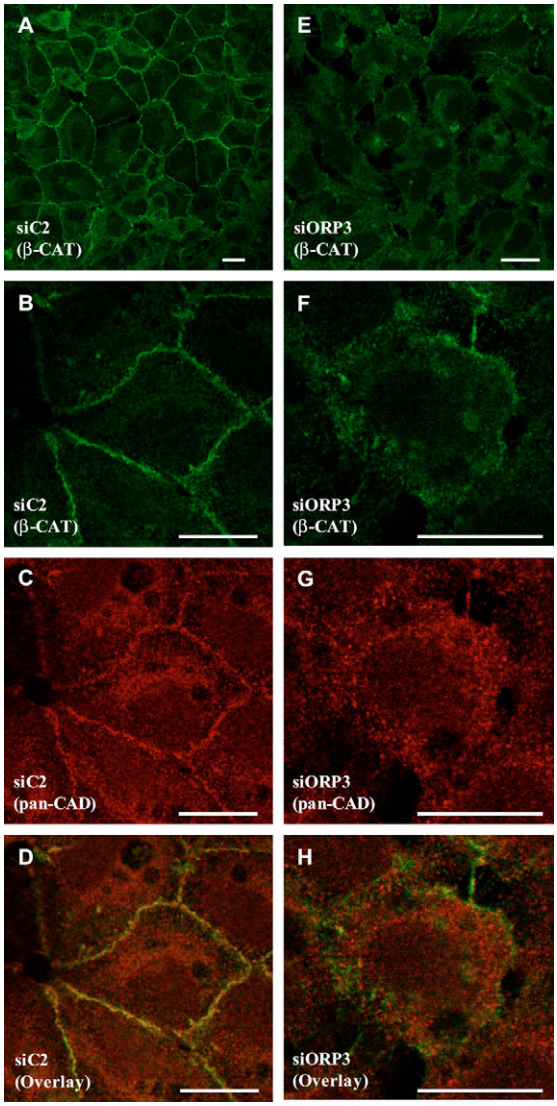

Fig. 6. Silencing of *ORP3* results in impaired cell-cell adhesion. HEK293 cells were transfected with control siC2 (A-D) or si*ORP3* (E-H). After 3 days, the cells were fixed and stained using anti-β-catenin (β-CAT) and anti-pan-cadherin (pan-CAD) antibodies. (A,E) β-catenin staining. (B-D,F-H) High-magnification images showing both β-catenin and pan-cadherin staining. Scale bars: 20 μm.

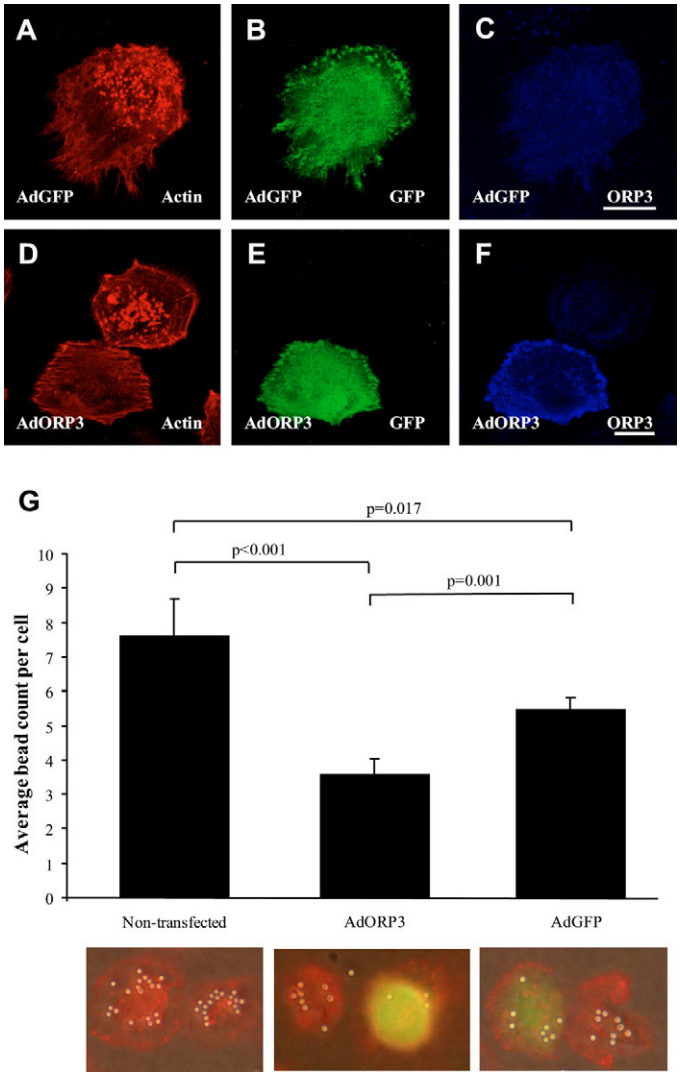

Fig. 7. Effects of ORP3 overexpression in human primary macrophages. Human primary macrophages were transduced with Ad*GFP* (A-C) or Ad*ORP3* (D-F) recombinant adenoviruses. After 72 hours, the cells were fixed and stained for F-actin (Actin) and ORP3 (ORP3). The GFP expressed from both adenoviruses is shown in green (GFP). Scale bars: 20 μm.
(G) Differentiated monocyte macrophages from three subjects were infected with Ad*ORP3* or Ad*GFP* for three days. Four million 3 μm polystyrene latex beads were loaded in each well containing ~200,000 cells. After 1 hour, the cells were fixed, stained with AF568P, photographed and the beads were counted. The data represent the number of beads per cell, mean (± s.e.m.); the number of cells analyzed: Control (n=2169), Ad*ORP3* (n=385), Ad*GFP* (n=885). The P values indicate statistical significance.

suspension cells (Zhang et al., 1996). When cells adhere to the extracellular matrix, R-Ras promotes adhesion-induced activation of the small GTPase Rac1 through its interaction partner PI3K (Marte et al., 1996; Holly et al., 2005). However, in addition to enhancement of matrix adhesion, overexpression of constitutively active R-Ras(38V) increases RhoA activity, resulting in a rounded non-polarized cell morphology and inhibition of cell migration (Zhang et al., 1996; Self et al., 2001; Jeong et al., 2005). R-Ras interacts with several effector proteins, most of which are shared by other members in the Ras family (Kinbara et al., 2003). The present finding that the inhibitory R-Ras(43N) mutant suppresses the morphological effect of ORP3 overexpression supports the notion that the two proteins are able to regulate integrins and the actin cytoskeleton. Although ORP3 forms a physical complex with the R-Ras, we do not know whether the interaction is direct. Furthermore, ORP3 interacted with both active and dominant inhibitory forms of the GTPase. Similarly, the adaptor protein Nck, which plays an important role in regulation of the actin cytoskeleton (Buday et al., 2002), interacts with both the active and inactive forms of R-Ras (Wang, B. et al., 2000).

During cell spreading, silencing of ORP3 expression enhanced cell adhesion to the extracellular matrix. This was accompanied by an increased spreading area and elevation of β1 integrin activity, whereas ORP3 overexpression resulted in a polarized protrusion phenotype accompanied with impaired cell spreading, decreased integrin activity and impaired macrophage phagocytic activity.

Exactly the opposite phenotypes have been reported in R-Ras(38V)-expressing cells: nonpolarized cell morphology, enhanced cell spreading, increased integrin activity and enhanced phagocytosis (Zhang et al., 1996; Self et al., 2001; Jeong et al., 2005; Wozniak et al., 2005; Ada-Nguema et al., 2006). Based on these observations, we find it likely that ORP3 regulates cell-matrix adhesion via modulation of integrin activity. Since overexpression of wild-type or mutant R-Ras also showed the previously reported effects on integrin activity in cells subjected to ORP3 silencing, it seems that ORP3 acts upstream of R-Ras. However, our results do not exclude the possibility that ORP3 and R-Ras could impact integrin activity via separate pathways.

We present evidence that ORP3 also influences cell-cell adhesion. Gene silencing of *ORP3* inhibited the formation of cell-cell contacts and the phosphorylation status of ORP3 was shown to depend on cell density. In HEK293 cells, endogenous ORP3 localized to the ER and thin filopodial projections of the plasma membrane. The existence of ORP3-positive projections, as well as the phosphorylation status of ORP3 depended strongly on the cell density. The phosphorylation status of ORP3 increased drastically with the loss of cell-matrix and cell-cell adhesion. Phosphorylation was downregulated when the cells grew firmly attached on substratum and further diminished when they reformed cell-cell contacts. At high cell density, the number of filopodial projections declined markedly and ORP3 existed mainly in the dephosphorylated form. Furthermore, disruption of cadherin-mediated cell-cell contacts through Ca^{2+} depletion resulted in increased phosphorylation of ORP3. Intriguingly, ORP3 phosphorylation was also induced by incubating HEK293 cells with antibodies against E-cadherin. This result suggests that antibody binding to E-cadherin triggers an outside-in signal, which promotes phosphorylation of ORP3 via an unknown mechanism. Cadherins play central roles in cell-cell adhesion and there is significant functional crosstalk between the cadherin and the integrin machineries (Chen and Gumbiner, 2006). Weakening of cell-cell adhesion and inhibition of cadherin function is suggested to enhance integrin function via a process involving the small GTPase Rap1, a member of the Ras superfamily (Balzac et al., 2005). The effects of ORP3 on cell-matrix and cell-cell adhesion are consistent with this model and suggest that ORP3 may modulate both integrin and cadherin function.

Is the interaction of ORP3 with R-Ras dependent on the ORP3 phosphorylation status? Fig. 3A shows that both the lower and the upper ORP3 bands are found in the anti-R-Ras immunoprecipitates, with the hypophosphorylated lower band form being more abundant. Since this form is also predominant in the overexpressed ORP3 protein pool, the only conclusion one can draw is that at least the hypophosphorylated form of ORP3 interacts efficiently with R-Ras. Whether the hyperphosphorylated form interacts more weakly with the GTPase is at this point unclear.

ORP3 expression is shown to have a strong impact on the actin cytoskeleton. During cell spreading, silencing of ORP3 influences the organization of F-actin in HEK293 cells. At early stages of the spreading process, control cells exhibited numerous filopodial extensions, whereas cells subjected to ORP3 silencing displayed abundant lamellipodia and defective filopodial extensions. Disturbance of the F-actin organization was also evident at the later stages of the spreading process. Control cells had compact cortical actin bundles located at close vicinity of the plasma membrane, whereas the *ORP3*-silenced cells showed a 'basket-like' actin network. Consistent with a functional connection between ORP3

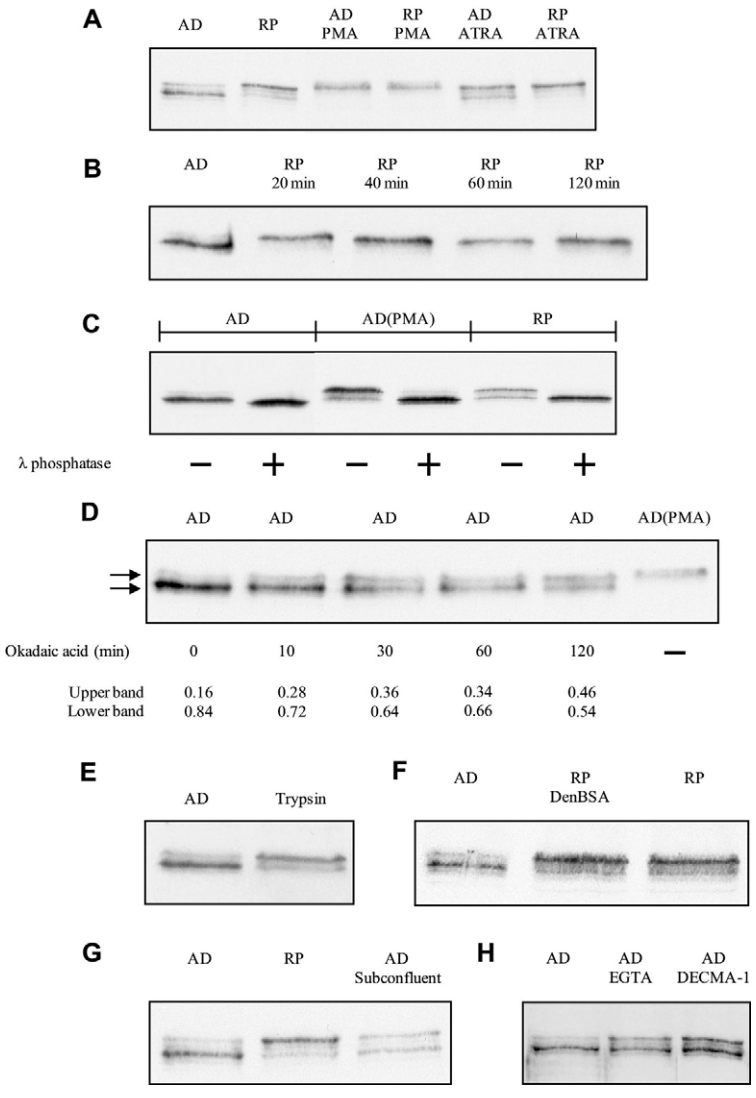

Fig. 8. ORP3 is phosphorylated depending on the cell-adhesion status. (A) HEK293 cells were cultured in normal medium for 20 hours. Confluent adherent (AD) cells were lyzed directly on the plate or trypsinized briefly and cells were allowed to adhere and spread on the fibronectin-coated plate in normal medium for 1 hour (replated cells, RP). Adherent and replated cells were treated with 100 nM phorbol myristate acetate (PMA) or 10 μM all-trans retinoic acid (ATRA) for 60 minutes before lysis. (B) A time course in which trypsinized cells were replated and allowed to adhere and spread for 20-120 minutes (indicated at the top). (C) Cells treated as specified above were lyzed and treated without and with λ-phosphatase (indicated at the bottom). (D) Confluent adherent cells treated with 50 nM okadaic acid for the indicated times. PMA-treated adherent cell sample was used as a positive control for the band shift to the upper position. Quantified intensities of the two ORP3 bands (arrows) are indicated at the bottom. (E) Trypsinized cells (Trypsin) washed and lyzed directly in SDS-PAGE loading buffer or (F) incubated for 1 hour on a dish treated with denatured BSA to inhibit adhesion (DenBSA). Adherent and replated cells are shown for a comparison. (G) Comparison of adherent and replated cells with those at 40-60% confluency (AD Subconfluent). (H) Adherent cells were treated with 5 mM EGTA (AD EGTA) or E-cadherin-blocking antibodies (AD DECMA-1) for 30 minutes.

and R-Ras, HEK293 cells transfected with constitutively active R-Ras(38V) exhibited a very similar basket-like actin phenotype (Wozniak et al., 2005). The predominant phenotypic effect of ORP3 overexpression in HEK293 cells was the formation of long protrusions, dependent on a functional ORP3 PH domain. The formation of such polarized protrusions is reminiscent of neurite growth. Especially when ORP3 was expressed under serum-free conditions, the tips of the protrusions exhibited resemblance to neuronal growth cones (data not shown). In neuronal cells, serum starvation has been shown to induce integrin-dependent neurite outgrowth, which is highly dependent on Ras-mediated PI3K, Cdc42 and Rac1 activation (Sarner et al., 2000). Recent studies have pointed out that HEK293 cells express several factors that are usually present only in cells of neuronal origin (Shaw et al., 2002; Nalvarte et al., 2004). Therefore, the membrane protrusions formed in HEK293 cells may bear resemblance to polarized neurites (Shaw et al., 2002; Nalvarte et al., 2004; Govek et al., 2005). In this context it is noteworthy that a close homolog of ORP3, ORP6, was identified as one of the fifteen proteins that promote the differentiation of neurons from murine embryonic stem cells (Falk et al., 2007).

Protrusion formation similar to that induced by ORP3 has been reported to occur upon overexpression of several other proteins, all of which represent regulators of the actin cytoskeleton: Cdc42 effector protein 1 (CEP1/MSE55) (Burbelo et al., 1999), ATP-binding cassette transporter-1 (ABCA1) (Wang, N. et al., 2000; Tsukamoto et al., 2001), calpain 2 (CAPN2) (Franco et al., 2004; Perrin et al., 2006), downstream of kinase 2 (Dok-2, Dok-R or FRIP) (Master et al., 2003) and c-Abl tyrosine kinase (Master et al., 2003). Dok-2 and c-Abl represent proteins associated with Nck (Master et al., 2001; Master et al., 2003), which is involved in the regulation of R-Ras function (Wang, B. et al., 2000) and the actin cytoskeleton (Buday et al., 2002). Nck binds to Wiskott-Aldrich syndrome protein (WASP), which controls the nucleation of actin filaments by the Arp2/3 complex (Buday et al., 2002). One can therefore envision that the ORP3-R-Ras interaction could impact on Nck and associated proteins, which play central roles in actin regulation. In primary macrophages, overexpression of ORP3 caused the disappearance of podosomal structures, resembling the phenotype described in patients with Wiskott-Aldrich syndrome (Linder et al., 1999; Linder and Aepfelbacher, 2003). The above findings support a role of ORP3 as a modulator of F-actin organization.

Small Ras superfamily GTPases are central regulators of vesicle transport, cell spreading, adhesion, migration and phagocytosis processes, which require fast and efficient modification of actin cytoskeleton and membrane structures (Kinbara et al., 2003). Recently, yeast *Saccharomyces cerevisiae* ORP proteins were shown to be required for the Cdc42p-dependent establishment of cell polarity. The ORPs were found to promote polarity by maintaining the proper localization of Rho and Rab GTPases and septins, as well as the secretory pathway function. In budding yeast, deletion of all *OSH* genes resulted in a significant defect in the polarized exocytosis of secretory vesicles (Kozminski et al., 2006). Therefore, ORP proteins could play an important role in regulatory processes that guide vesicular lipid/membrane transport to the sites of membrane growth. Of note, R-Ras has recently been shown to be involved in the regulation of RalA-mediated exocytosis of endosomal vesicles (Takaya et al., 2007). In addition to the interaction of ORP3 and R-Ras, we have recently shown that human ORP1L interacts with the small GTPase Rab7, a regulator of late-endosomal vesicle transport (Johansson et al., 2005; Johansson et al., 2007). The present functional evidence, together with the abundant expression of ORP3 in polarized cell types, suggests that this protein may play an important role in cell adhesion, spreading and polarization – processes involving dynamic F-actin reorganization and efficient directed membrane trafficking.

Members in the Ras GTPase superfamily, which regulate cell proliferation, adhesion, migration, vesicle transport and polarization processes, are frequently mutated in human cancer and leukaemia (Ehrhardt et al., 2002). Changes in gene expression during tumor progression are characteristically accompanied by alterations in cell-cell and cell-matrix adhesion (Christofori, 2006). ORP3 is frequently overexpressed in epithelial cancers and leukaemia and interacts with R-Ras. We propose that aberrantly high expression of ORP3 may modify the adhesion properties of cells in a manner that facilitates tumor progression.

Materials and Methods

Plasmids, siRNAs and antibodies

The human *ORP3* cDNA constructs in eukaryotic expression vector (pcDNA4/HismaxC) have been described previously (see supplementary material Fig. S2) (Lehto et al., 2005). Wild-type R-Ras(WT), active mutant R-Ras(38V) and inactive mutant R-Ras(43N) in pcDNA4/TO vector (Invitrogen) were kindly provided by Johan Peränen (Furuhjelm and Peränen, 2003). An *ORP3*-specific siRNA duplex (si*ORP3*) and scrambled control siRNA duplexes (siC1 and siC2) were used for silencing studies. Three silent mutations in the sequence corresponding to si*ORP3* were introduced into *ORP3* cDNA (*ORP3*mut) using the QuikChange site-directed mutagenesis kit (Stratagene) (see supplementary material Table S1). Anti-ORP3 polyclonal rabbit antibodies raised against an N-terminal peptide of human ORP3 (Lehto et al., 2004), were used for detection of endogenous ORP3 protein. Information on the other antibodies used is listed in supplementary material Table S2.

HEK293 cell culture and transfection

Human embryonic kidney (HEK293) cells were cultured in Eagle-MEM (Sigma-Aldrich) supplemented with 10% heat-inactivated fetal bovine serum (FBS), 10 mM HEPES pH 7.4, 1% non-essential amino acids (NEAA), 100 U/ml penicillin and 100 μg/ml streptomycin. Serum-free medium (Eagle-MEM, 10 mM HEPES pH 7.4 and 1% NEAA) was used in transfection. For morphological studies, HEK293 cells were plated on coverslips coated with 0.4% gelatin (Sigma-Aldrich), vitronectin (5 μg/ml in phosphate-buffered saline, PBS) (Sigma-Aldrich) or fibronectin (10 μg/ml in PBS) (Sigma-Aldrich). HEK293 cells were transfected with plasmid DNA or siRNA duplexes using Lipofectamine (LFA) 2000 (Invitrogen) reagent according to the manufacturer's instructions. The day before transfection, cells were cultured on plates/wells coated with 0.4% gelatin. In the case of 12-well culture plates, 800 ng plasmid DNA or 2 μg siRNA duplexes was used. Transfection time for plasmid DNA was 18-24 hours, resulting in approximately 100-fold ORP3 protein level compared with the endogenous amount. The siRNAs were transfected twice over a 3-day period.

Immunofluorescence microscopy

HEK293 and primary macrophages on coverslips were fixed with 2.6% paraformaldehyde, 160 mM HEPES (pH 7.4), 10 mM MES [2-(N-morpholino)-ethane sulphonic acid] buffer (pH 6.1), 320 mM sucrose, for 30-60 minutes. Immunofluorescence (IF) staining was performed as described earlier (Lehto et al., 2005). F-actin was stained using Oregon Green 488 (OG488P) or Alexa Fluor 568 Phalloidin (AF568P) according to the manufacturer's instructions (Molecular Probes). The specimens were analysed with a Leica TCS SP1 laser-scanning confocal microscope.

Immunoprecipitation

HEK293 cells cultured on 6 cm dishes were transfected with ORP3 and R-Ras(WT), R-Ras(38V), or R-Ras(43N) constructs. After transfection for 18 hours, the cells were lyzed in 0.5 ml lysis buffer (20 mM Tris-HCl pH 7.5, 150 mM NaCl, 2 mM $MgCl_2$, 10% glycerol, 0.5% NP-40). Undissolved material was collected by centrifugation (15 minutes, 16,100 ***g***, 4°C). Pellets were resuspended in 150 μl reducing Laemmli loading buffer, of which 10 μl was loaded on SDS-PAGE gels. The cleared lysates were pre-incubated with 50 μl 50% protein-G-Sepharose (PGS) 4 Fast Flow (GE Healthcare) at 4°C for 30 minutes. After a short centrifugation (1 minute, 400 ***g***), the supernatants were transferred into new tubes and incubated overnight with anti-R-Ras (1 μg) or irrelevant control (1 μg) rabbit IgG at 4°C. On the following day, immunocomplexes were precipitated by incubating samples with 50 μl 50% PGS for 6 hours at 4°C. After a short centrifugation, the unbound sample (~0.5 ml) was removed and 5 μl was used for SDS-PAGE. The matrices were then washed three times with the lysis buffer and immunocomplexes were eluted by boiling with 30 μl

Laemmli loading buffer, of which half was loaded on SDS-PAGE gels. ORP3 and R-Ras were detected with anti-Xpress and anti-R-Ras antibodies, respectively.

Cell-spreading experiments

HEK293 cells were cultured on gelatin-coated 3 cm dishes. Cells that had been growing on a plate for more than 20 hours were designated adherent cells. For spreading experiments, a new set of plates was incubated with fibronectin (10 μg/ml in PBS) overnight. On the next day, fibronectin solution was removed and the plates were incubated for 5 minutes at room temperature with 0.2% BSA in PBS. The cells were washed briefly with PBS and overlaid with 500 μl 0.05% trypsin-PBS (Difco) for 1-2 minutes. The detached cells were plated on fibronectin-coated plates in the presence of 2 ml normal culture medium. HEK293 cells were allowed to adhere and spread on the dishes for 20-120 minutes. Cells that have been trypsinized and allowed to spread on fibronectin-coated plates were designated replated cells. In some experiments adherent and replated cells were treated with the protein kinase C activators phorbol myristate acetate (PMA; 100 nM) and all-trans retinoic acid (ATRA; 10 μM) for 1 hour. All chemicals except trypsin were purchased from Sigma-Aldrich.

Cell-area measurements during adhesion and spreading

For silencing experiments, HEK293 cells were transfected twice with *ORP3* or control siRNAs over a 3-day period. For overexpression, HEK293 cells were transfected with *ORP3*/pcDNA4 plasmid or with an empty vector (Mock) for 20 hours. Untransfected HEK293 cells were also included for a comparison. Cells cultured on 12-well plates were washed once with PBS and trypsinized briefly. The detached cells were divided in three separate wells containing normal HEK293 culture medium and fibronectin/BSA-coated coverslips. After 1 hour, the cells were fixed and stained with OG488P. The endogenous or overexpressed ORP3 proteins were detected with anti-ORP3 or anti-Xpress antibodies, respectively. The area covered by the cells was determined from confocal microscope images using the Quantify functions of the Leica LCS software.

Cell-adhesion and β1 integrin activity assays

HEK293 cells were transfected either with siRNAs (si*ORP3*, siC2) or plasmid constructs as indicated. At 50 hours post transfection the cells were collected with trypsin-EDTA and resuspended into serum-free culture medium. For cell adhesion assays, 10,000 cells were allowed to adhere to collagen-coated 96-well plate wells for 1 hour. The cells were washed with PBS and fixed with 4% PFA in PBS. Adherent cells were stained with propidium iodide (0.3 μg/ml in PBS) and measured with Acumen Explorer Fluorescence Microplate Cytometer (TTP LabTech). For β1 integrin activity assays, 500,000 cells were incubated for 30 min at room temperature with active β1 integrin antibody P4G11 (1.0 μg/ml) or total β1 integrin antibody P5D2 (5 μg/ml) (supplementary material Table S2). The negative control was P4G11 with 2 mM EDTA. After secondary antibody incubation (anti-mouse Alexa Fluor 647), the cells were washed once with 1 ml PBS and analyzed with BD FACSArray Bioanalyzer (BD Biosciences).

Isolation and differentiation of human monocyte macrophages

Human monocytes were isolated from buffy coats obtained from the Finnish Red Cross Blood Transfusion Service (Helsinki, Finland) and differentiated into macrophages as previously described (Oksjoki et al., 2006).

Generation of recombinant adenoviruses

Human *ORP3* cDNA was cloned into pAdenovator-CMV5-IRES-GFP vector (Qbiogene). Recombinant *ORP3* adenovirus (Ad*ORP3*) was generated in HEK293 cells using the AdEasy system according to manufacturer's instructions. A control adenovirus encoding GFP alone (Ad*GFP*) was generated from the plain pAdenovator transfer vector. The recombinant viruses were plaque purified, expanded and purified on CsCl gradients as described previously (Laitinen et al., 1998).

Adenoviral transduction of macrophages

Differentiated monocyte macrophages cultured in 25 cm^2 bottles were trypsinized with 0.7 ml 0.05% trypsin, 0.5 mM EDTA pH 8.0 in PBS at 37°C for 25 minutes. Detached cells were resuspended in 2.8 ml medium C [RPMI 1640 (Sigma-Aldrich), 10% FBS, 10 mM HEPES, 0.03% glutamine, 1% NEAA, 100 U/ml penicillin and 100 μg/ml streptomycin] and counted. The cells were allowed to adhere to coverslips in multiwell plates at 37°C for 1 hour. Unbound cells were removed and fresh MF-SFM (Gibco-Invitrogen) containing the above antibiotics (medium B) was added to adherent cells. Primary macrophages were infected with Ad*ORP3* and Ad*GFP* at a MOI of 300 for 72 hours, resulting in a ~100-fold increase in the ORP3 protein level compared with the endogenous level.

Phagocytosis assay

Mononuclear cells derived from three different blood donors were isolated and differentiated into monocyte macrophages as described above. The macrophages were trypsinized, counted and divided on fibronectin-coated coverslips on 24-well plates (~200,000 cells/well). Each sample was analyzed in triplicate. Cells were infected with Ad*ORP3* and Ad*GFP* adenoviruses for 72 hours. Four million 3 μm polystyrene latex beads (Sigma-Aldrich) suspended in medium B were added in each well. After 1 hour, the cells were washed, fixed and stained with AF568P as described above. The cells were photographed with a digital camera attached to a Nikon Eclipse E600 phase-contrast microscope. The beads were photographed under phase contrast and the fluorescent markers using the appropriate fluorescence channels. In the case of adenovirally infected monocyte macrophages, only the cells with visible green fluorescence were counted. The phagocytosed beads were calculated from a minimum of ten merged photomicrograph images.

Analysis of ORP3 phosphorylation in HEK293 cells

HEK293 cells were cultured on 3 cm gelatin coated dishes for 20 hours. The adherent confluent cells were used as such or replated after brief trypsinization on fibronectin/BSA-coated dishes for 1 hour (designated as replated cells). In time-course experiments the replated cells were incubated for 20-120 minutes. In some experiments, cell-matrix adhesion of replated cells was inhibited by coating dishes with denatured BSA. Adherent and replated cells were treated with 100 nM PMA or 10 μM ATRA for 1 hour. The cells were lysed in 80 μl lysis buffer (10 mM HEPES pH 7.4, 0.1% NP-40, Roche proteinase inhibitor cocktail). The samples were treated with and without 800 U λ-phosphatase (New England Biolabs) in the reaction volume of 100 μl for 1 hour at 30°C. After treatment, the samples were boiled with 50 μl Laemmli loading buffer for 3 minutes.

Confluent adherent cells grown on 3 cm plates were treated with normal culture medium supplemented with 50 nM okadaic acid (Roche Diagnostics) for 10, 20, 60 and 120 minutes. After treatment, the cells were lysed in 150 μl of Laemmli loading buffer. Equal amounts of samples were loaded on SDS-PAGE gels. Intensities of protein bands were quantified by densitometric scanning (Scion Image for Windows, Scion Corporation). Confluent adherent cells in normal medium were treated for 30 minutes with 5 mM EGTA or with an antibody against E-cadherin (DECMA-1; supplementary material Table S2). The cells were harvested in Laemmli loading buffer for western analysis using anti-ORP3 antibodies

Statistical analysis

Statistical analysis was performed with the SPSS for Windows software (release 13.0, SPSS, Chicago, IL). $P<0.05$ (two-tailed) was considered statistically significant.

We are grateful to Pirjo Ranta, Seija Puomilahti, Suvi Sokolnicki, Mari Jokinen and Maija Atuegwu for excellent technical assistance. The Wihuri Research Institute is maintained by the Jenny and Antti Wihuri Foundation. This study was supported by following grants: The Academy of Finland (grants 206298, 113013, 118720), The Sigrid Juselius Foundation, The Finnish Foundation for Cardiovascular Research, The Magnus Ehrnrooth Foundation and The Finnish Society of Sciences and Letters (V.M.O.); The Finnish Kidney Foundation (P.I.); The Wilhelm and Else Stockmann Foundation and the Folkhälsan Research Foundation (P.-H.G.); The Emil Aaltonen Foundation and the Finnish Cancer Foundation (J.I.).

References

Ada-Nguema, A. S., Xenias, H., Sheetz, M. P. and Keely, P. J. (2006). The small GTPase R-RAS regulates organization of actin and drives membrane protrusions through the activity of PLCϵ. *J. Cell Sci.* **119**, 1307-1319.

Almstrup, K., Ottesen, A. M., Sonne, S. B., Hoei-Hansen, C. E., Leffers, H., Rajpert-De Meyts, E. and Skakkebaek, N. E. (2005). Genomic and gene expression signature of the pre-invasive testicular carcinoma in situ. *Cell Tissue Res.* **322**, 159-165.

Ando, T., Suguro, M., Kobayashi, T., Seto, M. and Honda, H. (2003). Multiple fuzzy neural network system for outcome prediction and classification of 220 lymphoma patients on the basis of molecular profiling. *Cancer Sci.* **94**, 906-913.

Balzac, F., Avolio, M., Degani, S., Kaverina, I., Torti, M., Silengo, L., Small, J. V. and Retta, S. F. (2005). E-cadherin endocytosis regulates the activity of Rap1: a traffic light GTPase at the crossroads between cadherin and integrin function. *J. Cell Sci.* **118**, 4765-4783.

Bijl, J., Sauvagenau, M., Thompson, A. and Sauvagenau, G. (2005). High incidence of proviral integrations in the Hoxa locus in a new model of E2a-PBX1-induced B-cell leukaemia. *Genes Dev.* **19**, 224-233.

Buday, L., Wunderlich, L. and Tamas, P. (2002). The Nck family of adapter proteins: regulators of actin cytoskeleton. *Cell. Signal.* **14**, 723-731.

Burbelo, P. D., Snow, D. M., Bahou, W. and Spiegel, S. (1999). MSE55, a Cdc42 effector protein, induces long cellular extensions in fibroblasts. *Proc. Natl. Acad. Sci. USA* **96**, 9083-9088.

Chen, X. and Gumbiner, B. M. (2006). Crosstalk between different adhesion molecules. *Curr. Opin. Cell Biol.* **18**, 572-578.

Chng, W. J., Schop, R., Price-Troska, T., Ghobrial, I., Kay, N., Jelinek, D. F., Gertz, M. A., Dispenzieri, A., Lacy, M., Kyle, R. A. et al. (2006). Gene expression profiling of Waldenström's macroglobulinemia reveals a phenotype more similar to chronic lymphocytic leukaemia than multiple myeloma. *Blood* **108**, 2755-2763.

Christofori, G. (2006). New signals from the invasive front. *Nature* **441**, 444-450.

Ehrhardt, A., Ehrhardt, G. R. A., Guo, X. and Schrader, J. W. (2002). Ras and relatives – job sharing and network keep an old family together. *Exp. Hematol.* **30**, 1089-1106.

Ek, S., Andreasson, U., Hober, S., Kampf, C., Ponten, F., Uhlen, M., Merz, H. and Borrebaeck, C. A. K. (2006). From gene expression analysis to tissue microarrays – a rational approach to identify therapeutic and diagnostic targets in lymphoid malignancies. *Mol. Cell. Proteomics* **5**, 1072-1081.

Falk, A., Karlsson, T. E., Kurdija, S., Frisen, J. and Zupicich, J. (2007). High-throughput identification of genes promoting neuron formation and lineage choice in mouse embryonic stem cells. *Stem Cells* **25**, 1539-1545.

Franco, S., Perrin, B. and Huttenlocher, A. (2004). Isoform specific function of calpain 2 in regulating membrane protrusion. *Exp. Cell Res.* **299**, 179-187.

Furuhjelm, J. and Peränen, J. (2003). The C-terminal end of R-RAS contains a focal adhesion signal. *J. Cell Sci.* **116**, 3729-3738.

Gashaw, I, Grummer, R., Klein-Hitpass, L., Dushaj, O., Bergmann, M., Brehm, R., Grobholz, R., Kliesch, S., Neuvians, T. P., Schmid, K. W. et al. (2005). Gene signatures of testicular seminoma with emphasis on expression of ets variant gene 4. *Cell. Mol. Life Sci.* **62**, 2359-2368.

Goldfinger, L. E., Ptak, C., Jeffery, E. D., Shabanowitz, J., Han, J., Haling, J. R., Sherman, N. E., Fox. J. W., Hunt, D. F. and Ginsberg, M. H. (2007). An experimentally derived database of candidate Ras-interacting proteins. *J. Proteome Res.* **6**, 1806-1811.

Govek, E.-E., Nevey, S. E. and Van Aelst, L. (2005). The role of the Rho GTPases in neuronal development. *Genes Dev.* **19**, 1-49.

Holly, S. P., Larson, M. K. and Parise, L. V. (2005). The unique N-terminus of R-Ras is required for Rac activation and precise regulation of cell migration. *Mol. Cell. Biol.* **16**, 2458-2469.

Jaworski, C. J., Moreira, E., Li, A., Lee, R. and Rodriguez, I. R. (2001). A family of 12 human genes containing oxysterol binding domains. *Genomics* **78**, 185-196.

Jeong, H.-W., Nam, J.-O. and Kim, I.-S. (2005). The COOH-terminal end of R-Ras alters the motility and morphology of breast epithelial cells through Rho/Rho-kinase. *Cancer Res.* **65**, 507-515.

Johansson, M., Bocher, V., Lehto, M., Chinetti, G., Kuismanen, E., Ehnholm, C., Staels, B. and Olkkonen, V. M. (2003). The two variants of oxysterol binding protein-related protein-1 display different tissue expression patterns, have different intracellular localization and are functionally distinct. *Mol. Biol. Cell* **14**, 903-915.

Johansson, M., Lehto, M., Tanhuanpää, K., Cover, T. L. and Olkkonen, V. M. (2005). The oxysterol-binding protein homologue ORP1L interacts with Rab7 and alters functional properties of late endocytic compartments. *Mol. Biol. Cell* **16**, 5480-5492.

Johansson, M., Rocha, N., Zwart, W., Jordens, I., Janssen, L., Kuijl, C., Olkkonen, V. M. and Neefjes, J. (2007). Activation of endosomal dynein motors by stepwise assembly of Rab7-RILP-p150Glued, ORP1L and the receptor {beta}lll spectrin. *J. Cell Biol.* **12**, 459-471.

Juric, D., Sale, S., Hromas, R. A., Yu, R., Wang, Y., Duran, G. E., Tibshirani, R., Einhorn, L. H. and Sikic, B. I. (2005). Gene expression profiling differentiates germ cell tumors from other cancer and defines subtype-specific signatures. *Proc. Natl. Acad. Sci. USA* **102**, 17763-17768.

Kinbara, K., Goldfinger, L. E., Hansen, M., Chou, F.-L. and Ginsberg, M. H. (2003). RAS GTPases: integrins' friends or foes? *Nat. Rev. Mol. Cell Biol.* **4**, 767-776.

Kozminski, K. G., Alfaro, G., Dighe, S. and Beh, C. T. (2006). Homologues of oxysterol-binding protein affects Cdc42p- and Rho1p-mediated cell polarization in Saccharomyces cerevisiae. *Traffic* **7**, 1224-1242.

Laitinen, M., Mäkinen, K., Manninen, H., Matsi, P., Kossila, M., Agrawal, R. S., Pakkanen, T., Luoma, J. S., Viita, H., Hartikainen, J. et al. (1998). Adenovirus-mediated gene transfer to lower limb artery of patients with chronic critical leg ischemia. *Hum. Gene Ther.* **9**, 1481-1486.

Lehto, M. and Olkkonen, V. M. (2003). The OSBP-related proteins: a novel protein family involved in vesicle transport, cellular lipid metabolism and cell signalling. *Biochim. Biophys. Acta* **1631**, 1-11.

Lehto, M., Laitinen, S., Chinetti, G., Johansson, M., Ehnholm, C., Staels, B., Ikonen, E. and Olkkonen, V. M. (2001). The OSBP-related protein family in humans. *J. Lipid Res.* **42**, 1203-1213.

Lehto, M., Tienari, J., Lehtonen, S., Lehtonen, E. and Olkkonen, V. M. (2004). Subfamily III of mammalian oxysterol-binding protein (OSBP) homologues: the expression and intracellular localization of ORP3, ORP6 and ORP7. *Cell Tissue Res.* **315**, 39-57.

Lehto, M., Hynynen, R., Karjalainen, K., Kuismanen, E., Hyvärinen, K. and Olkkonen, V. M. (2005). Targeting of OSBP-related protein 3 (ORP3) to endoplasmic reticulum and plasma membrane is controlled by multiple determinants. *Exp. Cell Res.* **310**, 445-462.

Linder, S. and Aepfelbacher, M. (2003). Podosomes: adhesion hot-spots of invasive cells. *Trends Cell Biol.* **13**, 376-385.

Linder, S., Nelson, D., Weiss, M. and Aepfelbacher, M. (1999). Wiskott-Aldrich syndrome protein regulates podosomes in primary human macrophages. *Proc. Natl. Acad. Sci. USA* **96**, 9648-9653.

Marte, B. M., Rodriquez-Viciana, P., Wennström, S., Warne, P. H. and Downward, J. (1996). R-Ras can activate the phosphoinositide 3-kinase but not the MAP kinase arm of the Ras effector pathways. *Curr. Biol.* **7**, 63-70.

Master, Z., Jones, N., Tran, J., Jones, J., Kerbel, R. S. and Dumont, D. J. (2001). Dok-R plays a pivotal role in angiopoietin-1-dependent cell migration through recruitment and activation of Pak. *EMBO J.* **20**, 5919-5928.

Master, Z., Tran, J., Bishnoi, A., Chen, S. H., Ebos, J. M. L., Van Slyke, P., Kerbel, R. S. and Dumont, D. J. (2003). Dok-R binds c-Abl and regulates Abl kinase activity and mediates cytoskeletal reorganization. *J. Biol. Chem.* **278**, 30170-30179.

Nalvarte, I., Damdimopoulos, A. E., Nyström, C., Nordman, T., Miranda-Vizuete, A., Olsson, J. M., Eriksson, L., Björnstedt, M., Arner, E. S. J. and Spyrou, G. (2004). Overexpression of enzymatically active human cytosolic and mitochondrial thioredoxin reduxtase in HEK293 cells. *J. Biol. Chem.* **279**, 54510-54517.

Oksjoki, R., Kovanen, P. T., Lindstedt, K. A., Jansson, B. and Pentikainen, M. O. (2006). OxLDL-IgG immune complexes induce survival of human monocytes. *Arterioscler. Thromb. Vasc. Biol.* **26**, 576-583.

Olkkonen, V. M., Johansson, M., Suchanek, M., Yan, D., Hynynen, R., Ehnholm, C., Jauhiainen, M., Thiele, C. and Lehto, M. (2006). The OSBP-related proteins (ORPs): global sterol sensors for co-ordination of cellular lipid metabolism, membrane trafficking and signaling processes. *Biochem. Soc. Trans.* **34**, 389-391.

Ozaki, T., Neumann, T., Wai, D., Schäfer, K.-L., Valen, F., Lindner, N., Scheel, C., Böcker, W., Winkelmann, W., Dockhorn-Dworniczak, B. et al. (2003). Chromosomal alterations in osteosarcoma cell lines revealed by comparative genomic hybridization and multicolour karyotyping. *Cancer Genet. Cytogenet.* **140**, 145-152.

Perrin, B. J., Amann, K. J. and Huttenlocher, A. (2006). Proteolysis of cortactin by calpain regulates membrane protrusion during cell migration. *Mol. Biol. Cell* **17**, 239-250.

Sander, B., Flygare, J., Porwit-MacDonald, A., Smith, C. I., Emanuelsson, E., Kimby, E., Liden, J. and Christensson, B. (2005). Mantle cell lymphomas with low levels of cyclin D1 long mRNA transcripts are highly proliferative and can be elevated cyclin A2 and cyclin B1. *Int. J. Cancer* **117**, 418-430.

Sarner, S., Kozma, R., Ahmed, S. and Lim, L. (2000). Phosphatidyl 3-kinase, Cdc42 and Rac1 act downstream of Ras in integrin-dependent neurite outgrowth in NIE-115 neuroblastoma cells. *Mol. Cell. Biol.* **20**, 158-172.

Self, A. J., Caron, E., Paterson, H. F. and Hall, A. (2001). Analysis of R-Ras signalling pathways. *J. Cell Sci.* **114**, 1357-1366.

Shaw, G., Morse, S., Ararat, M. and Graham, F. L. (2002). Preferential transformation of human neuronal cells by adenoviruses and the origin of HEK293 cells. *FASEB J.* **16**, 869-871.

Sperger, J. M., Chen, X., Draper, J. S., Antosiewicz, J. E., Chon, C. H., Jones, S. B., Brooks, J. andrews, P. W., Brown, P. O. and Thomson, J. A. (2003). Gene expression patterns in human embryonic stem cells and human pluripotent germ cell tumors. *Proc. Natl. Acad. Sci. USA* **100**, 13350-13355.

Staub. E., Gröne, J., Mennerich, D., Röpcke, S., Klamann, I., Hinzmann, B., Castano-Velez, E., Mann, B., Pilarsky, C., Brummendorf, T. et al. (2006). A genome-wide map of aberrantly expressed chromosomal islands in colorectal cancer. *Mol. Cancer* **5**, 1-44.

Takaya, A., Kamio, T., Masuda, M., Mochizuki, N., Sawa, H., Sato, M., Nagashima, A., Matsuno. A., Kiyokawa, E. and Matsuda, M. (2007). R-RAS regulates exocytosis by Rgl2/Rlf-mediated activation of RalA on endosomes. *Mol. Biol. Cell* **18**, 1850-1860.

Tsafrir, D., Bacolod, M., Selvanayagam, Z., Tsafrir, I., Shia, J., Zeng, Z., Liu, H., Krier, C., Stengel, R. F., Barany, F. et al. (2006). Relationship of gene expression and chromosomal abnormalities in colorectal cancer. *Cancer Res.* **66**, 2129-2137.

Tsukamoto, K., Hirano, K., Tsujii, K., Ikegami, C., Zhongyan, Z., Nishida, Y., Ohama, T., Matsuura, F., Yamashita, S. and Matsuzawa, Y. (2001). ATP-binding cassette transporter-1 induces rearrangement of actin cytoskeletons possibly through Cdc42/-WASP. *Biochem. Biophys. Res. Commun.* **287**, 757-765.

Tuomisto, T. T., Riekkinen, M. S., Viita, H., Levonen, A.-L. and Ylä-Herttuala, S. (2005). Analysis of gene and protein expression during monocyte-macrophage differentiation and cholesterol loading – cDNA and protein array study. *Atherosclerosis* **180**, 283-291.

Wang, B, Zou, J. X., Ek-Rylander, B. and Ruoslahti, E. (2000). R-Ras contains a proline-rich site that binds to SH3 domains and is required for integrin activation by R-Ras. *J. Biol. Chem.* **275**, 5222-5227.

Wang, N., Silver, D. L., Costet, P. and Tall, A. R. (2000). Specific binding of ApoA-I enhanced cholesterol efflux and altered plasma membrane morphology in cells expressing ABC1. *J. Biol. Chem.* **275**, 33053-33058.

Wheelock, M. J. and Johnson, K. R. (2003). Cadherins as modulators of cellular phenotype. *Annu. Rev. Cell Dev. Biol.* **19**, 207-235.

Wozniak, M. A., Kwong, L., Chodniewicz, D., Klemke, R. L. and Keely, P. J. (2005). R-Ras controls membrane protrusion and cell migration through the spatial regulation of Rac and Rho. *Mol. Biol. Cell* **16**, 84-96.

Yamada, S, Kohu, K., Ishii, T, Ishidoya, S., Kanto, M. S., Fukuzaki, A., Adachi, Y., Endoh, M., Mori, T., Sasaki, H. et al. (2004). Gene expression profiling identifies a set of trancripts that are up-regulated in human testicular seminoma. *DNA Res.* **11**, 335-344.

Zhang, Z., Vuori, K., Wang, H., Reed, J. C. and Ruoslahti, E. (1996). Integrin activation by R-Ras. *Cell* **85**, 61-69.

Table S1. Sequences of the siRNAs and mutagenesis primers

Name	Sequence (sense strand)
siORP3	CGGCACCUAUUUGGAACUUdTdT
siC1	CGAUGUCAUCUUUUGAGGCdTdT
siC2	UAGCGACUAAACACAUCAAdTdT
siORP3b-mutagenesis*	GGTGAGCAACGGCACCTATcTaGAgCTTAGAAAAGATCTTGGTTT

*For creating ORP3mut cDNA construct. Lowercase letters indicate positions of silent mutations.

Table S2. Primary antibodies used in this study

Antibody	Cat. no./ product code	Manufacturer
Anti-β-Actin (clone JLA20), Mab*	---	Developmental Studies Hybridoma Bank (Univ. of Iowa)
Anti-β1-integrin (P4G11), Mab	---	Developmental Studies Hybridoma Bank (Univ. of Iowa)
Anti-β1-integrin (P2D2), Mab	---	Developmental Studies Hybridoma Bank (Univ. of Iowa)
Anti-β-Catenin, Mab	610153	BD Transduction Laboratories
Anti-pan-Cadherin, Rab**	71-7100	Zymed
Anti-CD68 (clone PG-M1), Mab	M0876	Dako
Anti-Cortactin (p80/85; clone 4F11), Mab	05-180	Upstate
Anti-E-Cadherin (clone DECMA-1), rMab***	U3254	Sigma-Aldrich
Anti-PDI, Mab	SPA-891	Stressgen
Anti-R-Ras, (C-19) Rab	sc-523	Santa Cruz Biotechnology
Anti-R-Ras (E-18), Mab	sc-32029	Santa Cruz Biotechnology
Anti-Xpress™, Mab	R910-25	Invitrogen

* Mouse monoclonal antibody, **Rabbit polyclonal antibody, ***Rat monoclonal antibody